

A simple method of searching for a fixed solution in a coordinate domain

Sławomir Cellmer (✉ slawomir.cellmer@uwm.edu.pl)

University of Warmia and Mazury

Research Article

Keywords: GNSS data processing, Ambiguity Function, integer least-squares, Voronoi cells, precise satellite positioning

Posted Date: January 31st, 2022

DOI: <https://doi.org/10.21203/rs.3.rs-1301987/v1>

License:  This work is licensed under a Creative Commons Attribution 4.0 International License.

[Read Full License](#)

1 A simple method of searching for a fixed solution in a coordinate domain.

2

3 Sławomir Cellmer*¹, Krzysztof Noweł², Artur Fischer³

4 * e-mail: slawomir.cellmer@uwm.edu.pl; ORCID: 0000-0002-2614-8017

5 ^{1,2,3} Department of Geodesy, Univ. of Warmia and Mazury, 1 Oczapowskiego Str., 10-719 Olsztyn, Poland

6

7

8

9 **Abstract** Recently, more and more Global Navigation Satellite Systems satellites are available
10 for observation. Apart from obvious advantages, this brings new challenges in developing
11 efficient computational methods of processing signals obtained from more satellites than to
12 date. From the viewpoint of computation process efficiency, the most critical step is ambiguity
13 resolution. Because of the discrete character of ambiguities, the search procedure is employed
14 to perform this task. The search space dimension significantly impacts a search procedure
15 computational load. The time needed for obtaining a solution raises considerably when the
16 search space dimension is greater. Therefore, the improved version of the well-known concept
17 of searching for a fixed solution in a three-dimensional coordinate domain was proposed and
18 tested. The math model of the proposed approach is presented together with the algorithm of
19 the search procedure. The numerical experiments were designed for simulated and real data.
20 The simulated data has been prepared based on the concept proposed by the authors. This data
21 simulation method is described in detail. The test results confirmed the reduction of the time
22 needed to obtain the results when the proposed method is applied. This advantage over
23 traditional methods unveils in the case of many satellites. Moreover, the real-data test pointed
24 out that using the new approach is beneficial in reducing the computation time also in the case
25 of a few satellites if long sessions are processed.

26

27 **Keywords** GNSS data processing · Ambiguity Function · integer least-squares · Voronoi cells
28 · precise satellite positioning

29

30

31 **Introduction**

32 The Global Navigation Satellite Systems (GNSS) growth brings both new opportunities and
33 challenges in signal processing methods. The apparent advantage of the increasing number of

34 satellites possible to observe is the rise in the number of observations collected by the GNSS
35 receiver. On the other hand, besides new signals, each new satellite provides new unknown
36 values, i.e., ambiguities to be estimated. The rise in amounts of parameters substantially
37 impacts the computational load. Even the most popular and efficient methods of optimizing the
38 computational process in the classic approach, for example, in the LAMBDA method
39 (Teunissen, 1995, 1999; de Jonge and Tiberius, 1996; Liu et al., 1999; Chang et al., 2005;
40 Zhou 2011; Xu, 2012) are sensitive to the number of ambiguities. Xu proved that if observed
41 satellites exceed a specific number, even the most efficient decorrelation techniques do not
42 improve the search procedure efficiency (Xu, 2001). If there is more than a specific number of
43 satellites, the decorrelation procedure takes more time than the search procedure performed
44 without such a transformation. Thus, the cost of the enhancement technique outnumbers the
45 benefits that are got from it! Therefore, it is justified to reconsider the concept of searching for
46 integer ambiguities in a coordinate domain. The search space dimension is constant and
47 amounts to three in such a case. Thus, the search space dimension does not depend on the
48 number of satellites. Consequently, the computational load of a search procedure does not rise
49 with increasing the number of satellites. It can even decrease if a search region is set correctly.
50 Usually, the search region is formed based on the float position covariance matrix. In that case,
51 this region shrinks with an increasing number of satellites because this typically improves
52 satellites' configuration geometry and float solution precision. Then, fewer candidates are
53 needed for carrying out the search procedure. The concept of searching for a fixed solution in
54 the coordinate domain dates back to the early years of satellite navigation system development.
55 Its classic form utilizes the Ambiguity Function (AF) method in the computation process. The
56 AF method of processing the GPS carrier phase observations was the first time proposed by
57 Counselman and Gourevitch (1981) and then by Remondi (1984). A substantial improvement
58 of the AF method has been proposed by Cellmer et al. (2010). They developed the Modified
59 Ambiguity Function Approach (MAFA). A description of the MAFA method can be found in,
60 for example, (Cellmer 2012 2013 2015; Cellmer et al. 2010 2017 2018 2021; Kwasniak et al.
61 2016 2017; Baselga 2010; Nowel et al. 2018). Some researchers use the MAFA method
62 foundations in recent research in airplane attitude determination (Wang et al. 2007; Wang et
63 al. 2019; Wu et al. 2019, Zhao et al., 2022). Nevertheless, we do not use the functional model
64 of the MAFA method in the present contribution. Unlike the MAFA, all formulas used in the
65 search procedure proposed in this article are based solely on the float solution results. In
66 contrast, the MAFA method requires the whole carrier phase data set for forming the
67 observation equations when testing the candidates. Still, however, we take advantage of the
68 other solutions used in the MAFA method: creating the search region in the coordinate domain
69 and setting an optimal search step (Cellmer et al. 2018, 2021). The search region is in the form

70 of an error ellipsoid of the approximate position, and the optimal search step's length derivation
71 is based on a concept of the Voronoi cells (VC) and an actual satellites' configuration.
72 According to Hassibi and Boyd (1998), the Voronoi cell of the point X_0 in a lattice is the set of
73 points in space closer to X_0 than to any other point in the lattice. Xu (2006) used the VC to
74 analyze an ambiguity resolution problem. In Teunissen's integer equivariant estimation theory,
75 the VC is called an "in-pull region," where distance accounts for the non-Euclidean metric
76 (Teunissen, 1999, 2003). Cellmer et al. (2021) used the VC in the meaning of a region
77 containing candidates that give the same solution from the methods based on searching for a
78 fixed solution in a coordinate domain. This meaning of the VC is assumed in our work. The
79 search step's length resulting from the method proposed by Cellmer et al. (2021) is the longest
80 distance between neighboring candidates that one at the same time guarantees we do not skip
81 any VC included in the search region. In contrast to the MAFA method, the search procedure
82 proposed in this contribution does not need the whole data set to test successive candidates.
83 The search procedure is conducted based on approximate position coordinates and their
84 covariance matrix. Both magnitudes are obtained from a float solution.

85 In the next section, the classic form of the mixed integer-real least squares estimation math
86 model is introduced to familiarize readers with the notation used in this work. The third section
87 is devoted to the main topic of this work, i.e., the search procedure in a coordinate domain
88 (SinCD). Sole results from a float solution are used in this procedure as input. Two types of
89 computational experiments are described in the fourth section. They are based on real and
90 simulated data. The results of those experiments illustrate the effects of the proposed method.
91 The conclusions are presented in the last section.

92

93 **The classic approach of precise positioning**

94 The math model of precise satellite positioning is (Hoffman-Wellenhof et al., 2008; Leick et
95 al., 2015):

$$96 \quad \mathbf{y} = \mathbf{A}\mathbf{a} + \mathbf{B}\mathbf{b} + \mathbf{e} \quad (1)$$

97 where \mathbf{y} is the data vector, \mathbf{a} is the integer ambiguity vector, \mathbf{b} is the real parameter vector, \mathbf{A}
98 and \mathbf{B} are the corresponding design matrices, and \mathbf{e} is the noise vector. The \mathbf{y} vector consists of
99 double differenced (DD) carrier phase observations and/or code observations. The \mathbf{b} vector
100 consists of the baseline components. Sometimes it can also contain other parameters, e.g.,
101 atmospheric corrections. The classic approach of precise satellite positioning consists of the
102 three stages:

103 1) The least-squares (LS) solution in which the integer nature of ambiguities is discarded. This
 104 solution is called the "float solution."

105 2) The integer ambiguity resolution. This stage also includes a validation of the results.

106 3) The solution with integer ambiguities. This solution is called the "fixed solution."

107 The LS estimates of the \mathbf{a} and \mathbf{b} vectors, in the first stage, are obtained from:

$$108 \quad \begin{bmatrix} \hat{\mathbf{a}} \\ \hat{\mathbf{b}} \end{bmatrix} = \begin{bmatrix} \mathbf{Q}_{\hat{\mathbf{a}}} & \mathbf{Q}_{\hat{\mathbf{a}}\hat{\mathbf{b}}} \\ \mathbf{Q}_{\hat{\mathbf{b}}\hat{\mathbf{a}}} & \mathbf{Q}_{\hat{\mathbf{b}}} \end{bmatrix} \begin{bmatrix} \mathbf{A}^T \mathbf{P}_y \mathbf{y} \\ \mathbf{B}^T \mathbf{P}_y \mathbf{y} \end{bmatrix} \quad (2)$$

$$109 \quad \text{where: } \begin{bmatrix} \mathbf{Q}_{\hat{\mathbf{a}}} & \mathbf{Q}_{\hat{\mathbf{a}}\hat{\mathbf{b}}} \\ \mathbf{Q}_{\hat{\mathbf{b}}\hat{\mathbf{a}}} & \mathbf{Q}_{\hat{\mathbf{b}}} \end{bmatrix} = \begin{bmatrix} \mathbf{A}^T \mathbf{P}_y \mathbf{A} & \mathbf{A}^T \mathbf{P}_y \mathbf{B} \\ \mathbf{B}^T \mathbf{P}_y \mathbf{A} & \mathbf{B}^T \mathbf{P}_y \mathbf{B} \end{bmatrix}^{-1} \quad \text{and } \mathbf{P}_y \text{ is the observation weight matrix.}$$

110 The LS estimator of the integer ambiguity vector is defined as:

$$111 \quad \tilde{\mathbf{a}} = \arg \min_{\mathbf{z} \in \mathbb{Z}^n} \|\hat{\mathbf{a}} - \mathbf{z}\|_{\mathbf{Q}_{\hat{\mathbf{a}}}}^2 \quad (3)$$

112 The expression at the $\arg \min(\cdot)$ operator denotes a weighted norm of the $(\hat{\mathbf{a}} - \mathbf{z})$ vector:

$$113 \quad \|\hat{\mathbf{a}} - \mathbf{z}\|_{\mathbf{Q}_{\hat{\mathbf{a}}}}^2 = (\hat{\mathbf{a}} - \mathbf{z})^T \mathbf{Q}_{\hat{\mathbf{a}}}^{-1} (\hat{\mathbf{a}} - \mathbf{z}) \quad (4)$$

114 It is necessary to employ the search procedure since the solution domain of formula (3) has a
 115 discrete character. The ambiguity resolution step is always associated with the validation of the
 116 results. The last step in precise positioning is a "fixed solution," which incorporates the integer
 117 ambiguities obtained in the previous step:

$$118 \quad \tilde{\mathbf{b}} = \hat{\mathbf{b}} - \mathbf{Q}_{\hat{\mathbf{b}}\hat{\mathbf{a}}} \mathbf{Q}_{\hat{\mathbf{a}}}^{-1} (\hat{\mathbf{a}} - \tilde{\mathbf{a}}) \quad (5)$$

119 The critical part of this three-step approach of precise positioning is the step of ambiguity
 120 resolution. To date, many improvements to the search procedure have been developed and
 121 successfully applied in practice. However, still, the search procedure is conducted in n -dim
 122 ambiguity space. The concept of moving the search procedure from the n -dim ambiguity space
 123 to the 3-dim coordinate space is presented in the next section.

124

125 **The search procedure in a coordinate domain**

126 The conditional solution (5) derived from model (2) describes the change of the \mathbf{b} vector
 127 resulting from the modification of the \mathbf{a} vector. The method proposed in this work utilizes the
 128 relationship of type (5) but with swapped the \mathbf{a} and \mathbf{b} vectors. This modification also concerns
 129 corresponding cofactor matrices. The conditional solution resulting from the model (2) can be

130 alternatively formulated as the change of the \mathbf{a} vector resulting from the change of the \mathbf{b} vector.

131 Such a formula can be derived using block matrix:

$$132 \quad \mathbf{T} = \begin{bmatrix} \mathbf{I} & -\mathbf{Q}_{\hat{\mathbf{a}}\hat{\mathbf{b}}} \mathbf{Q}_{\hat{\mathbf{b}}}^{-1} \end{bmatrix} \quad (6)$$

133 where the first block \mathbf{I} is an identity matrix. Premultiplying normal equation system (2) by the

134 \mathbf{T} matrix, we get the formula for the $\hat{\mathbf{a}}$ vector conditioned by the $\hat{\mathbf{b}}$ vector:

$$135 \quad \hat{\mathbf{a}} = \left(\mathbf{Q}_{\hat{\mathbf{a}}} - \mathbf{Q}_{\hat{\mathbf{a}}\hat{\mathbf{b}}} \mathbf{Q}_{\hat{\mathbf{b}}}^{-1} \mathbf{Q}_{\hat{\mathbf{b}}\hat{\mathbf{a}}} \right) \mathbf{A}^T \mathbf{P}_y \mathbf{y} + \mathbf{Q}_{\hat{\mathbf{a}}\hat{\mathbf{b}}} \mathbf{Q}_{\hat{\mathbf{b}}}^{-1} \hat{\mathbf{b}} \quad (7)$$

136 Thus the change in the \mathbf{b} vector, such as, e.g., $\tilde{\mathbf{b}} = \hat{\mathbf{b}} + \Delta\mathbf{b}$ results in the modification of the \mathbf{a}
137 vector:

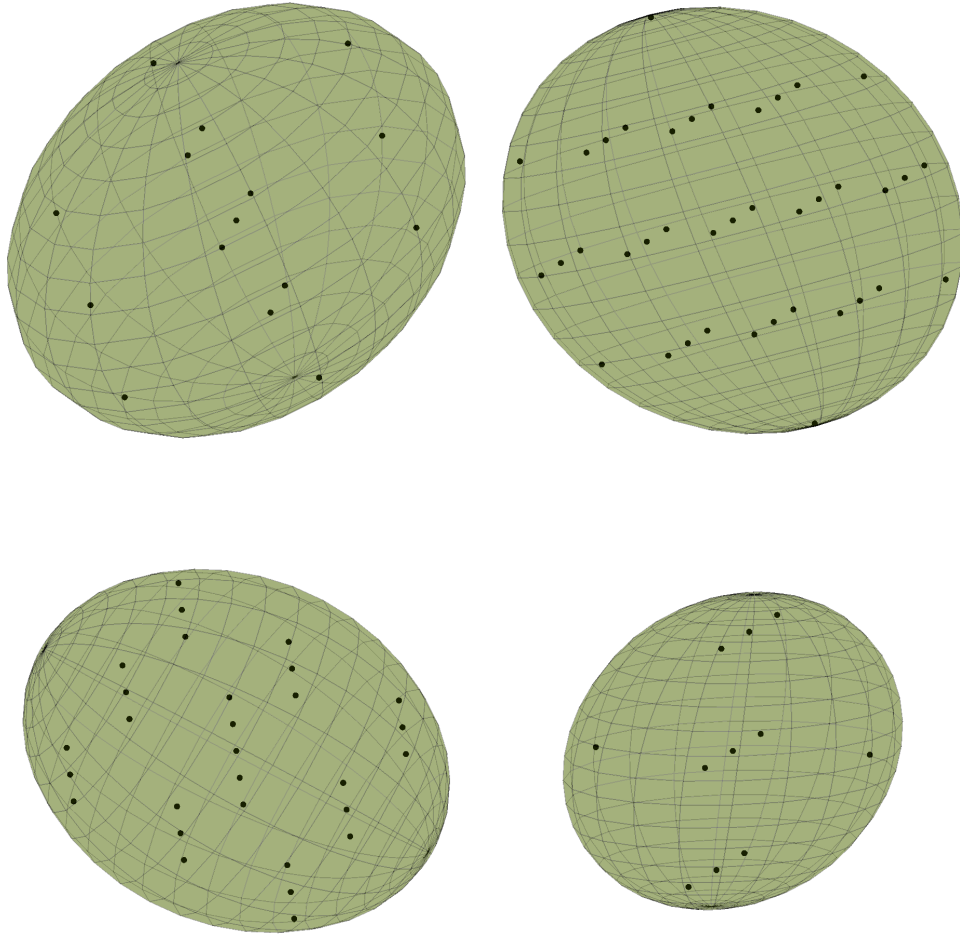
$$138 \quad \tilde{\mathbf{a}} = \left(\mathbf{Q}_{\hat{\mathbf{a}}} - \mathbf{Q}_{\hat{\mathbf{a}}\hat{\mathbf{b}}} \mathbf{Q}_{\hat{\mathbf{b}}}^{-1} \mathbf{Q}_{\hat{\mathbf{b}}\hat{\mathbf{a}}} \right) \mathbf{A}^T \mathbf{P}_y \mathbf{y} + \mathbf{Q}_{\hat{\mathbf{a}}\hat{\mathbf{b}}} \mathbf{Q}_{\hat{\mathbf{b}}}^{-1} \tilde{\mathbf{b}} \quad (8)$$

139 The difference of the equations (7) and (8) leads to:

$$140 \quad \tilde{\mathbf{a}} - \hat{\mathbf{a}} = \mathbf{Q}_{\hat{\mathbf{a}}\hat{\mathbf{b}}} \mathbf{Q}_{\hat{\mathbf{b}}}^{-1} (\tilde{\mathbf{b}} - \hat{\mathbf{b}}) \quad (9)$$

141 The description of applying the above formula in the proposed method is presented in the
142 further part of this section. This method is carried out according to the following steps: forming
143 a search region in coordinate space, subsequently establishing a grid of candidates inside it,
144 then testing each candidate and choosing this, which best satisfies the criterion assumed on the
145 tests' stage. Although the main stages of the proposed approach are similar to those in the
146 classic approach, the details differ significantly. The proposed method assumes that the float
147 solution is obtained the same way as the traditional approach. Next, the search region, as the
148 confidence region of the float solution, is established. In the 3-dim coordinate space, this region
149 takes the form of an error ellipsoid of an approximate position from the float solution. The
150 initial candidates (IC) grid is formed inside the search space. The arrangement of the IC set has
151 to guarantee that no the VC of integer ambiguity vector located inside the search region is
152 omitted. On the other hand, to satisfy the computational efficiency, the distance between
153 neighboring IC should be as long as possible so that the number of IC is small. The rules of
154 forming the search region and setting the grid of IC inside it, which account above conditions,
155 are described in detail by Cellmer et al. (2021). Figure 1 shows some examples of an
156 arrangement of IC inside the error ellipsoid. The examples are taken from the tests described
157 in the last section of the article. The essence of the proposed method is included in the next
158 step of the data processing. Let us name the ICs with \mathbf{b}_{IC} . For i -th \mathbf{b}_{IC} we compute the
159 corresponding ambiguity vector:

$$160 \quad \mathbf{a}_{ICi} = \hat{\mathbf{a}} - \mathbf{Q}_{\hat{\mathbf{a}}\hat{\mathbf{b}}} \mathbf{Q}_{\hat{\mathbf{b}}}^{-1} (\hat{\mathbf{b}} - \mathbf{b}_{ICi}) \quad (10)$$



162 **Fig. 1** Examples of the arrangements of the initial candidates inside the error ellipsoid.

163

164 Each ambiguity vector obtained by (10) is rounded to the nearest integer vector:

$$165 \quad \mathbf{a}_{FCi} = \text{round}(\mathbf{a}_{ICi}) \quad (11)$$

166 The integer vector \mathbf{a}_{FCi} corresponds to the i -th final candidate. Each vector \mathbf{a}_{FCi} is tested to find

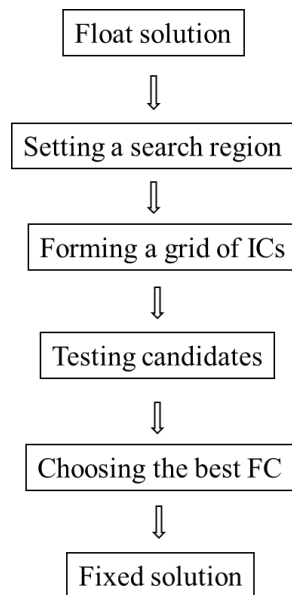
167 that one which minimizes criterion:

$$168 \quad \mathbf{a}_{FC\min} = \arg \min_{\mathbf{z} \in \mathbb{Z}^n} \|\hat{\mathbf{a}} - \mathbf{a}_{FCi}\|_{\mathbf{Q}_a}^2 \quad (12)$$

169 The $\mathbf{a}_{FC\min}$ vector is employed to compute the final solution:

$$170 \quad \mathbf{b}_{fix} = \hat{\mathbf{b}} - \mathbf{Q}_{\hat{\mathbf{b}}\hat{\mathbf{a}}} \mathbf{Q}_{\hat{\mathbf{a}}}^{-1} (\hat{\mathbf{a}} - \mathbf{a}_{FC\min}) \quad (13)$$

171 The successive steps of the computational process are depicted in Figure 2. The first three steps
172 of the computation process were discussed in (Cellmer et al., 2018; 2021). The primary issue
173 of the proposed method is included in the fourth step of the computational process: ICs testing.
174



176 **Fig. 2** Computational process of precise positioning based on search procedure in coordinate
177 domain

178 This step comprises operations (10) and (11), and also computing the norm on the right hand
179 of formula (12). Note the number of ICs can be greater than the number of FCs. The rules of
180 setting optimal search steps guarantee that no integer candidate is skipped. On the other hand,
181 a few ICs may fall into the same VC and consequently give the same FC. This is the cost of
182 reducing the dimension of a search space and has no significant impact on a computational load
183 if a search step length is set correctly.

184

185 **Numerical experiments**

186 *The real data test*

187 The first experiment is based on real data collected in two permanently operating EUREF
188 stations: WTZR and WTZZ (Germany), on 12, May, 2019, during a 24 h observation session.
189 The subject of the experiment is to test the performance of the new search procedure. The
190 analysis compares the new method with the classic one implemented in the LAMBDA method.
191 In the latter approach, a search for a fixed solution conducts in an ambiguity domain. The very
192 short baseline (1.62 m) was chosen for the tests to avoid any impact of atmospheric delays as
193 extraneous factors irrelevant in comparative analysis. Such a short baseline lets to take the

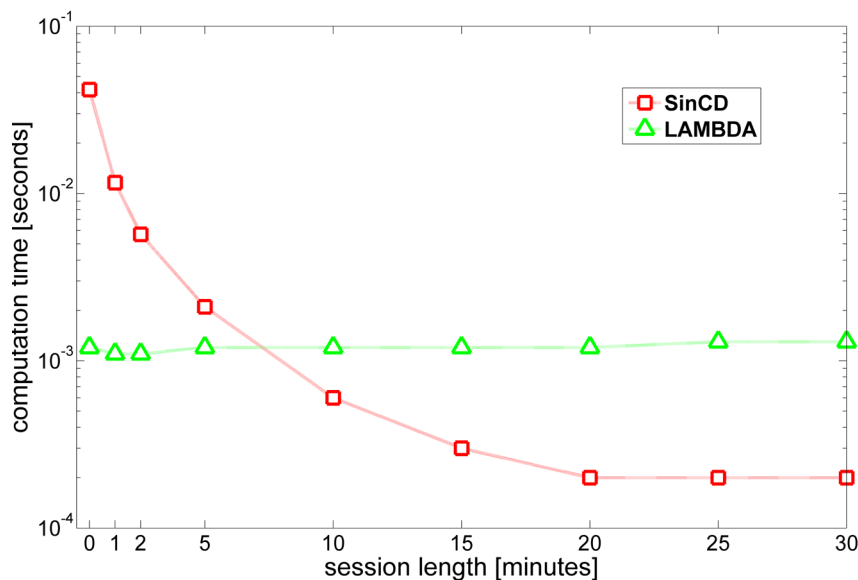
194 assumption that all atmospheric delays are eliminated by forming double differences of
195 observations. Only the single-frequency GPS signals were processed in the experiment. The
196 data used in this test was already utilized in another experiment, described by Cellmer et al.
197 (2021). The interval between consecutive epochs was 30 seconds. The WTZR was set as a
198 reference station and the WTZZ as a rover. The precise position of the rover was computed
199 based on the data collected in a 24h session. This position was used as a reference for further
200 comparisons. Next, the whole observation set was divided into short observation sessions. The
201 2000 subsequent epochs at 30-second intervals from the beginning of the 24h observation
202 session were adopted as the starting epochs for the successive short sessions. The tests were
203 carried out for sessions of various lengths: from a single-epoch solution to 30 minutes sessions.
204 There were 2000 separate sessions tested for each session length. There were 7 satellites in
205 most sessions. Only in some cases were observations collected from 8 satellites. The
206 approximate position in each session was obtained using the DD code and phase observations
207 discarding the integer nature of ambiguities (the float solution). The error ellipsoid of the
208 approximate position was formed using the covariance matrix from a float solution and setting
209 the confidence level to 0.999. The final precise position was estimated using two approaches.
210 The first way is the method proposed in the article and the second way is the LAMBDA
211 method. For simplicity, the first approach is denoted as #1 and the second as #2. The results
212 were compared. In the second approach, the computations were conducted using the Matlab
213 function *LAMBDA_06.m* retrieved from the TU Delft website:
214 [https://www.tudelft.nl/citg/over-faculteit/afdelingen/geoscience-remote-](https://www.tudelft.nl/citg/over-faculteit/afdelingen/geoscience-remote-sensing/research/lambda/lambda)
215 [sensing/research/lambda/lambda](https://www.tudelft.nl/citg/over-faculteit/afdelingen/geoscience-remote-sensing/research/lambda/lambda) (LAMBDA method, 2021). Table 1 lists the solutions'
216 success rates (SR) in both approaches. The SR values were computed separately for each
217 session length. The ambiguities obtained from 24h session were assumed to be actual.

218 **Table 1** Success rates as a percentage of correct solutions in the samples of 2000 observation sessions

	Session length [minutes]							
	Single-epoch	1	2	5	10	15	20	30
	Success rates [%]							
#1 (SinCD)	45.6	59.8	70.2	85.3	94.8	98.2	98.6	100.0
#2 (LAMBDA)	45.2	60.7	72.4	90.0	99.8	100.0	100.0	100.0

219
220 Thus, the tested short-session solutions containing the actual ambiguity values are considered
221 the correct solutions. The SR values are expressed in the percentage of correct solutions among
222 2000 sessions with a given length. The differences in SR ranged from 0 (for 30 min sessions)
223 to 5 (for 10 min sessions). The proposed method achieved higher SR for single-epoch solutions.
224 In other cases, better SR was obtained by the LAMBDA method. Although the percentage of

225 correct solutions is not precisely the same in both approaches, the differences in their values
 226 are minor. The mean value of absolute differences in SR in both approaches is 2.0%. The core
 227 element of the analysis is a comparison of the time needed for finding the correct solution in
 228 both approaches. Figure 3 depicts the mean computation time computed from 2000 sessions
 229 separately for each session length. On the X-axis are session lengths expressed in minutes,
 230 whereas on the Y-axis is a computation time in seconds. The log scale has been applied on the
 231 Y-axis. The session length has no impact on computation time in the LAMBDA method. Its
 232 value amounts slightly over 10^{-3} seconds for all session lengths.



234 **Fig. 3** Relationship between a session length and a computation time in the SinCD and the
 235 LAMBDA methods.

236 At the same time, the impact of session length on computation time is significant in the SinCD
 237 method. Its value ranges from $0.2 \cdot 10^{-3}$ (for the longest sessions) to $41.8 \cdot 10^{-3}$ in the case of
 238 single-epoch positioning. Shorter computation time in the SinCD method than in the LAMBDA
 239 is for 10-minute and longer sessions. In the present case study, the number of satellites amounts
 240 to 7 or, in some sparse sessions, 8. A relationship between the number of satellites and a
 241 computation time in both approaches can be evaluated based on simulated data. The following
 242 experiment has been designed for this purpose.

243

244 *The test based on simulated data*

245 It has been assumed that the positioning was conducted based on single-epoch data. The
 246 computations were repeated 2000 times for each assumed number of satellites. The satellite
 247 distribution was generated randomly in each epoch.

248 The simulated code-observations set can be modeled using simulated observation residuals:

$$249 \quad \nabla\Delta\mathbf{P} = \nabla\Delta\boldsymbol{\rho}^{(\text{actual})} + \nabla\Delta\mathbf{v}_c \quad (14)$$

250 or using simulated shift between approximated position and actual position

$$251 \quad \nabla\Delta\mathbf{P} = \nabla\Delta\boldsymbol{\rho}^{(\text{actual})} + \delta\boldsymbol{\rho} \quad (15)$$

252 where: $\nabla\Delta\mathbf{P}$ is double differenced (DD) code-observations vector, $\nabla\Delta\mathbf{v}_c$ is DD code-
 253 observation residuals vector, $\nabla\Delta\boldsymbol{\rho}^{(\text{actual})}$ is DD actual geometric distances vector, $\delta\boldsymbol{\rho}$ is a part
 254 of a computed DD geometric distance, resulting from a shift of approximated position regard
 255 to the actual one. The last term in (11) can be expressed in linear form as:

$$256 \quad \delta\boldsymbol{\rho} = \mathbf{A}\mathbf{d}\mathbf{x} \quad (16)$$

257 where the \mathbf{A} matrix is a design matrix of DD code-observations.

258 Subtracting (15) from (14) and inserting (16) we get observation equations for simulated code-
 259 data:

$$260 \quad \nabla\Delta\mathbf{v}_c = \mathbf{A}\mathbf{d}\mathbf{x} \quad (17)$$

261 in which the $\nabla\Delta\boldsymbol{\rho}^{(\text{actual})}$ and the $\nabla\Delta\mathbf{P}$ vectors vanish. All terms of (17) are prepared in the
 262 simulation procedure. Each entry of the $\nabla\Delta\mathbf{v}_c$ vector on the left side of equation (17) is formed
 263 by generating four residuals with assumed normal distribution $N[0, \sigma_c]$ where σ_c is the standard
 264 deviation of code-observations and then forming single and double differences. Four residuals
 265 have to be generated because this amount of pseudo-ranges is needed to create a single DD
 266 observation. The entries of the $\mathbf{d}\mathbf{x}$ vector are values generated from the range of plus/minus a
 267 few meters. Preparing a design matrix \mathbf{A} for simulated data set does not require knowledge
 268 about exact satellite positions. The j th row of the undifferenced design matrix \mathbf{A}_u consist of the
 269 ratios of components of satellite-rover distance and this distance:

$$270 \quad \mathbf{A}_u(j, :) = \left[-\frac{\Delta x_{rov}^j}{\rho_{rov}^j}, -\frac{\Delta y_{rov}^j}{\rho_{rov}^j}, -\frac{\Delta z_{rov}^j}{\rho_{rov}^j} \right] \quad (18)$$

271 That vector can be alternatively expressed by azimuth Az_j and elevation angle El_j in a local,
 272 horizontal coordinate system:

$$273 \quad \mathbf{A}_u(j, :) = \left[-\cos(El_j)\cos(Az_j), -\cos(El_j)\sin(Az_j), -\sin(El_j) \right] \quad (19)$$

274 Thus, it is enough to generate satellites' azimuths and elevation angles to form a design matrix
 275 for undifferenced observations. The \mathbf{A} matrix for DD observations is created by subtracting the
 276 row related to the reference satellite from the other rows of the \mathbf{A}_u matrix:

$$277 \quad \mathbf{A}(j,:) = \mathbf{A}_u(j,:) - \mathbf{A}_u(ref,:), \text{ for all } j \neq ref. \quad (20)$$

278 Thus, a design matrix for simulated data is formed using satellites' azimuths and elevations
 279 generated in ranges $(0;2\pi)$ and $(0;\pi/2)$ respectively. The observation equations for the
 280 simulated carrier phase observations can be derived analogously. They take the form similar to
 281 those of the equation (17):

$$282 \quad \nabla \Delta \mathbf{v}_{ph} = \frac{1}{\lambda} \mathbf{A} \mathbf{d} \mathbf{x} + \mathbf{a} \quad (21)$$

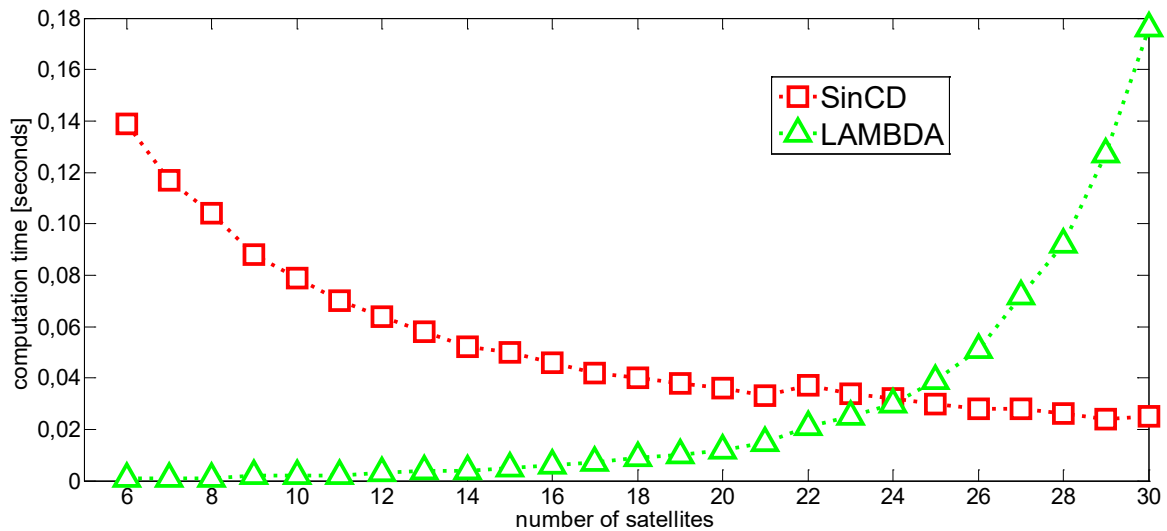
283 The only difference is an additional term of the ambiguity vector \mathbf{a} , which must be generated
 284 as a random integer number. The DD carrier phase residuals on the left hand are expressed in
 285 cycles, so the first term on the right hand is divided by carrier phase wavelength λ . There were
 286 considered the various number of satellites in a single-epoch positioning. The computations
 287 were repeated 2000 times for each number of satellites. Data were simulated and processed
 288 separately in each epoch using two approaches: the SinCD and the LAMBDA methods. The
 289 single-epoch positioning was conducted in a two-stage process: In the first stage, the
 290 observation set consisted of both types of code- and phase observations. The float solution
 291 results, not satisfying the integer nature of ambiguities, were the same in the two approaches.
 292 The precise position (fixed solution) was computed using the SinCD and LAMBDA methods.
 293 The SRs calculated from 2000 repetitions achieve almost the same values in both approaches
 294 for all tested numbers of satellites. The only difference in those values occurs in the case of 9
 295 satellites and amounts to 0.1% (99.9% in the SinCD method and 100% in the LAMBDA
 296 method). Table 2 lists the SR values for both methods with respect to the number of satellites.
 297 Since the SR for the number of satellites in the range of 10-30 achieves the same values
 298 amounting to 100.0% they have been placed in the single column.

299 **Table 2** Success rates as a percentage of correct solutions in 2000 repetitions of single-epoch positioning for
 300 various numbers of satellites

	Number of satellites				
	6	7	8	9	10-30
	Success rates [%]				
#1 (SinCD)	37.4	84.4	99.0	99.9	100.0
#2 (LAMBDA)	37.4	84.4	99.0	100.0	100.0

301
 302 Figure 4 depicts the computation time (CT) needed to obtain a solution by two tested methods.
 303 The CT was computed as a mean value from 2000 repetitions for each of the assumed numbers

304 of satellites. The CT of the LAMBDA method for the number of satellites fewer than 10 is
 305 stable and low. In contrast, the computational time of the SinCD method significantly
 306 decreases, in this range, when the number of satellites increases. The opposite situation starts
 307 when the number of satellites amounts to 20 or more. The computational time of the LAMBDA
 308 method starts to increase considerably, whereas the computational time of the SinCD method
 309 decreases gradually. Starting from 25 satellites providing the observations for a single-epoch
 310 positioning, the computational time of processing data is shorter in the SinCD method than in
 311 the LAMBDA method.



313 **Fig. 4** The computation time of the SinCD and the LAMBDA methods for a various number
 314 of satellites. The single-epoch positioning was performed based on simulated data.

315
 316 The results of the tests confirmed the good performance of the proposed method.
 317 Unfortunately, based on the real data test, we should admit that the SR is slightly fewer than in
 318 the traditional method in the cases with a small number of satellites and short observation
 319 sessions. However, the difference is not significant. On the other hand, for sessions 10-minute
 320 and longer with 7 or 8 satellites providing observation set, the CT is shorter in the proposed
 321 method than in the traditional one. Based on the test with simulated data, one can conclude that
 322 in a case of a single-epoch positioning, the CT is shorter in the proposed method than in the
 323 traditional one if the number of satellites is greater than 24.

324
 325 **Conclusions**

326 The motivation of the work was the apparent finding that the dimension of the search space is
 327 non-negligible for search procedure efficiency. The time needed for obtaining a solution raises
 328 considerably when the search space dimension is greater. Therefore, the concept of searching

329 for a fixed solution in a coordinate domain instead of in an ambiguity domain was investigated.
330 As a result, the new method was developed and tested. A major advantage of the proposed
331 method is moving a search procedure from multi-dimensional ambiguity space to only three-
332 dimensional coordinate space. Such an operation allows shortening computation time, thereby
333 increasing the efficiency of the precise positioning. This feature reveals oneself in the case of
334 an observation set obtained from many satellites. It has great importance in the prospect of
335 increasing the number of satellites resulting from developing modern satellite navigation
336 systems. The test results confirmed shortening computation time when using the proposed
337 method and that its advantage over traditional methods unveils in the case of many satellites.
338 The real data test pointed out that applying the new approach is beneficial in the case of long
339 sessions, even if we deal with a small number of satellites.

340

341 **Acknowledgments** This research was supported by the National Science Centre, Poland, grant
342 number 2018/31/B/ST10/00262.

343

344 **References**

- 345 Baselga S. (2010) Global optimization applied to GPS positioning by ambiguity functions.
346 Meas Sci Technol 21(12):125102, DOI: <http://dx.doi.org/10.1088/0957-0233/21/12/125102>
- 347 Cellmer S (2012) A graphic representation of the necessary condition for the MAFA method.
348 IEEE T Geosci Remote 50(2):482–488
- 349 Cellmer S (2013) Search procedure for improving modified Ambiguity Function Approach.
350 Surv Rev 45(332):380–385
- 351 Cellmer S (2015) Validation procedure in the Modified Ambiguity Function Approach.
352 Geodynamica et Geomaterialia 12(178):135–144
- 353 Cellmer S, Wielgosz P, Rzepecka Z (2010) Modified Ambiguity Function Approach for GPS
354 carrier phase positioning. J Geodesy 84(4):264–275
- 355 Cellmer S, Nowel K, Kwasniak D (2017) Optimization of a grid of candidates in the search
356 procedure of the MAFA method. In: Environmental Engineering 10th International
357 Conference, April 27-28 2017, Vilnius, Lithuania
- 358 Cellmer S, Nowel K, Kwaniak D (2018) The new search method in precise GNSS positioning.
359 IEEE T Aero Elec Sys 54(1):404–415

360 Cellmer S, Nowel K, Fischer A. (2021) A search step optimization in an ambiguity function-
361 based GNSS precise positioning. *Surv Rev*, DOI: 10.1080/00396265.2021.1885947

362 Chang X, Yang X, Zho T (2005) MLAMBDA: a modified LAMBDA method for integer least
363 squares estimation. *J Geodesy* 79(9):552–565

364 Counselman C, Gourevitch S (1981) Miniature interferometer terminals for earth surveying:
365 ambiguity and multipath with the global positioning system. *IEEE T Geosci Remote*
366 19(4):244–252

367 de Jonge PJ, Tiberius CCJM (1996) The LAMBDA method for integer ambiguity estimation:
368 implementation aspects. Publications of the Delft Computing Centre, LGR-Series No. 12

369 Hassibi A, Boyd S (1998) Integer parameter estimation in linear models with applications to
370 GPS. *IEEE T Signal Proces* 46(11):2938–2952

371 Hofmann-Wellenhof B., Lichtenegger H., Wasle E. (2008) GNSS-Global Navigation Satellite
372 Systems - GPS, GLONASS, Galileo & more. Springer-Verlag, Vienna, 2008.

373 Kwasniak D, Cellmer S, Nowel K (2016) Schreiber's differencing scheme applied to carrier
374 phase observations in the MAFA method. In: Proceedings of 2016 Baltic Geodetic Congress
375 (BGC Geomatics), pp. 197-204

376 Kwasniak D, Cellmer S, Nowel K (2017) Single frequency RTK positioning using Schreiber's
377 differencing scheme. In: 2017 Baltic Geodetic Congress (BGC Geomatics), Gdansk, Poland,
378 pp. 307–311

379 LAMBDA method from TU Delft (Accessed May 9, 2021, at <https://www.tudelft.nl/citg/over->
380 [faculteit/afdelingen/geoscience-remote-sensing/research/lambda/lambda](https://www.tudelft.nl/citg/over-faculteit/afdelingen/geoscience-remote-sensing/research/lambda/lambda))

381 Leick, A., Rapoport, L., Tatarnikov, D. (2015) GPS Satellite Surveying (4th edn). John Wiley
382 and Sons, Hoboken, New Jersey.

383 Liu LT, Hsu HT, Zhu YZ, Ou JK (1999) A new approach to GPS ambiguity decorrelation J
384 *Geodesy* 73:478–490

385 Nowel K, Cellmer S, Kwasniak D (2018) Mixed integer-real least squares estimation for
386 precise GNSS positioning using a Modified Ambiguity Function Approach. *GPS solut*
387 22(31):1–11, DOI 10.1007/s10291-017-0694-6

388 Remondi B (1984) Using the Global Positioning System (GPS) phase observable for relative
389 geodesy: modeling, processing and results. PhD thesis, Center for Space Research,
390 University of Texas at Austin

- 391 Teunissen P (1995) The least-squares ambiguity decorrelation adjustment: a method for fast
392 GPS integer ambiguity estimation. *J Geodesy* 70(1-2):65–82
- 393 Teunissen, P. (1999) An optimality property of the integer least-squares estimator. *J*
394 *Geodesy* 73, 587–593 <https://doi.org/10.1007/s001900050269>
- 395 Teunissen, P. (2003) Theory of integer equivariant estimation with application to GNSS. *J*
396 *Geodesy* 77, 402–410. <https://doi.org/10.1007/s00190-003-0344-3>
- 397 Wang Y, Zhan X, Zhang Y (2007) Improved ambiguity function method based on analytical
398 resolution for GPS attitude determination. *Meas Sci Technol* 18(9):2985–2990
- 399 Wang Y, Zhao X, Pang C, Wang X, Wu S, Zhang C (2019) Improved pitch-constrained
400 ambiguity function method for integer ambiguity resolution in BDS/MIMU-integrated
401 attitude determination. *J Geodesy* 93(4):56–572, DOI 10.1007/s00190-018-1182-7
- 402 Wu H, Zhao X, Pang C, Zhang L, Feng B (2019) Multivariate constrained GNSS real-time full
403 attitude determination based on attitude domain search. *J Navigation* 72(2):483–502, DOI
404 10.1017/S0373463318000784
- 405 Xu P (2001) Random simulation and GPS decorrelation *J Geodesy* 75(7-8): 408-423
- 406 Xu P (2006) Voronoi cells, probabilistic bounds, and hypothesis testing in mixed integer linear
407 models. *IEEE T Inform Theory* 52(7):3122–3138
- 408 Xu P (2012) Parallel Cholesky-based reduction for the weighted integer least squares problem
409 *J Geodesy* 86(1):35–52
- 410 Zhou Y (2011) A new practical approach to GNSS high-dimensional ambiguity decorrelation
411 *GPS Solut* 15:325–331
- 412 Zhao Y, Zou J, Zhang P, Guo J, Wang X, Huang G. (2022) An Optimization Method of
413 Ambiguity Function Based on Multi-Antenna Constrained and Application in Vehicle
414 Attitude Determination. *Micromachines*; 13(1):64. <https://doi.org/10.3390/mi13010064>
- 415



SLAWOMIR CELLMER received the Ph.D. degree in geodesy in 2002 from the University of Warmia and Mazury in Olsztyn, Poland. In 2013 he received habilitation (postdoctoral degree). He is an Associate Professor at the Faculty of Geoengineering at the University of Warmia and Mazury in Olsztyn (UWM), Poland. His research interests cover computational methods and GNSS data processing.



KRZYSZTOF NOWEL is an Assistant Professor at the Faculty of Geoengineering at the University of Warmia and Mazury in Olsztyn (UWM), Poland, where he earned his Ph.D. in Geodesy in 2015. His research interests include deformation measurement analysis and GNSS integer ambiguity resolution.



ARTUR FISCHER is a Ph.D. candidate at the Faculty of Geoengineering at the University of Warmia and Mazury in Olsztyn (UWM), Poland. His research interests contain computational methods in GNSS and engineering surveys.